Organic & Biomolecular Chemistry

Accepted Manuscript

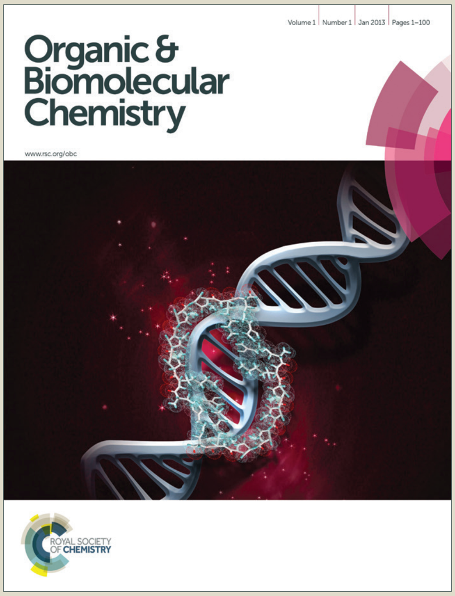

ROYAL SOCIETY OF CHEMISTRY

www.rsc.org/obc

Tuning of colour and chemical stability of model boranils: a strong effect of structural modifications

Grzegorz Wesela-Bauman,[a,b] * Mateusz Urban,[a] Sergiusz Luliński,[a] * Janusz Serwatowski,[a] Krzysztof Woźniak [b]

[a] *Physical Chemistry Department, Faculty of Chemistry, Warsaw University of Technology, Noakowskiego 3, 00-664 Warsaw, Poland*
[b] *Laboratory of Crystallochemistry, Department of Chemistry, University of Warsaw, Pasteura 1, 02-093 Warsaw, Poland.*

*Corresponding authors: grzegorz.wesela@chem.uw.edu.pl, serek@ch.pw.edu.pl

Keywords

borinic derivatives, boranils, fluorescence, structure-properties relationship, Hammett NMR correlations, Hammett UV-Vis correlations, charge density distribution, QTAIM analysis

Abstract

A series of diarylborinic complexes with salicydeneaniline ligands bearing various functional groups at the 6-position, have been synthesized with high yields by applying a straightforward one-pot multicomponent protocol. UV-Vis measurements revealed the influence of electronic character of substituents on the observed maximum of emission (λ_{em}). This has been confirmed by a relatively strong linear correlation ($R^2 = 0.92$) of λ_{em} with Hammett σ_p^+ constants. Such correlation was investigated using QTAIM analysis of charge density distribution. Absorption and emission bands for the obtained systems span between 390–437 nm and 506-590 nm, respectively, with quantum yields reaching 17%. Time-dependent UV-Vis absorption measurements revealed that diphenylborinic salicydeneaniline complexes undergo slow degradation in solution under ambient conditions. In contrast, the use of a naphthalene-based chromophore or introduction of fluorinated phenyl groups at the boron atom resulted in stable systems.

Introduction

Borinic complexes with various chelating ligands proved to be good materials for application in organic light emitting devices (OLEDs).[1–10] They can also be useful as dyes for medicinal purposes including bioimaging and diagnostics.[11] Optical properties of such complexes can be tuned mainly through the proper choice of a ligand acting as a chromophore. Ligand functionalization is additional and useful tool to influence colour and improve quantum yield of emission (Φ) of such systems.[2,12–16] Moreover, we have proved that different crystal packing induced by either compression in diamond anvil cells or through crystallization of different polymorphs can be used to improve charge transport properties (which is very important from the standpoint of application in light emitting devices).[17,18] There is a wide selection of available structures, but among them borinic complexes with (O,N)-chelating ligands are extensively studied, presumably due to their relatively high (in most cases) stability. Specifically, borinic complexes with 8-oxyquinolinato (Q) ligands were recognized as promising materials for application in optoelectronics. However, an access to many functionalized Q ligands is challenging which significantly limits the synthetic potential of this group of complexes.[19–21] Boron complexes with various salicylaldimine ligands, often termed *boranils* (**Figure 1**), represent their close analogues as they also possess phenolate oxygen and imine nitrogen atoms coordinated to the central B atom by means of covalent and dative bonds, respectively. However, in contrast with Q complexes featuring a central 5-membered ring, they chelate a boron atom to produce a six-membered heterocycle. In general, the synthesis of salicylaldimine chelating ligands is simple and efficient. This allows for broader structural modifications in comparison with the Q ligands. In addition, some obtained systems present a very interesting topology (*e.g.*, tris(ferrocene)-based systems with three-fold symmetry or stackable supramolecular crystal structures).[22,23]

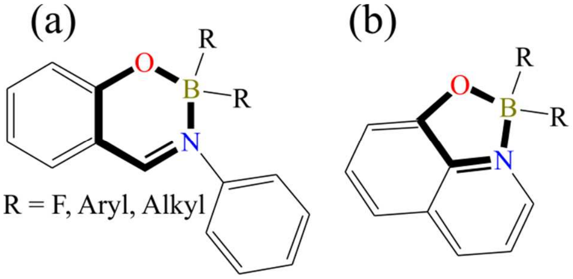

Figure 1. A six-membered *boranil* (a) and a five-membered 8-oxyquinolinato borinic complex (b).

According to the review article by Rao *et al.*,[3] the key role of the boron atom is to stabilize an anionic chelating (O,N)-ligand, which is consistent with lowering of the LUMO level. Hence, the stability of the B-N and B-O bonds is crucial for maintaining desired optical properties. Recently, Frath *et al.* presented a push-pull system, which was subjected to chemical functionalization without any disruption of the boron chelate ring.[24] Moreover, the emission of this dye was strongly enhanced once it was grafted onto a protein reaching the quantum yield (Φ) of 47%. The same group reported analogous *boranils* with even higher Φ values (up to 61%).[25]

The majority of reported examples of *boranils* contain the BF_2 unit as they can be readily prepared by the treatment of a free salicylaldimine ligand with the commercially available reagent $BF_3·Et_2O$. Related complexes bearing various diarylborinic moieties were studied less extensively than BF_2 derivatives as BAr_2 units need to be synthesized prior to the final complexation step. An exception is the parent BPh_2 group which can be delivered using commercially available BPh_3. However, that particular synthetic approach is not efficient.[26] Recently, we have made an effort in expanding the chemistry of heteroleptic borinic derivatives.[2,17,18,26] We observed that the character of aryl groups attached to the boron centre can influence optical (quantum yield of emission) and other physicochemical (*e.g.*, charge transport) properties.[27] Therefore, there is still a need for diverse modifications of aromatic rings attached to the boron atom. In addition, the appropriate functionalization of aryl groups opens a possibility of further transformations including polymerization, interaction with metal centres through coordination, H-bonding etc.[2,28–33] It should be noted that complexes with dialkylborinic moieties proved not suitable for the preparation of monolayers for optoelectronic devices though thermal evaporation techniques due to their low melting points.[28]

In this contribution, we present an improved synthetic protocol as well as a detailed physicochemical analysis of a series of functionalized diphenylborinic salicylidenaniline chelates. We have also found that the fluorination of phenyl groups at the boron atom has a strong impact on their chemical stability and can also be exploited for tuning their optical properties.

Results and discussion

Synthesis and characterization. We have developed a straightforward multicomponent one-pot protocol for the high-yield preparation of complexes **1-10** (**Scheme 1** & **2**). Diarylborinic precursors Ar_2BOR (Ar = Ph, 2,6-$F_2C_6H_3$, C_6F_5; R = Et, *i*-Pr) were obtained *via* reactions of aryllithiums ArLi with respective arylboronic esters $ArB(OR)_2$ followed by treatment with HCl (2 M solution in Et_2O). Finally, a 5-substituted salicylaldehyde and aniline were added simultaneously. The resulting mixture was then refluxed to give colourful solids with high yields (85-97%). The advantage of this procedure is based on the fact that it is not necessary to obtain and isolate salicydeneanilines and diarylborinic derivatives prior to the final boron chelation.

We have decided to broaden our work by investigation of complexes with modified organic ligands attached to the boron atom. Therefore, we have replaced the phenyl with 2,6-difluorophenyl and pentafluorophenyl groups. Compounds **9** and **10** were obtained using a multicomponent procedure similar to that described for compounds **1-8** (**Scheme 2**). The relatively low yield of **10** (31%) was probably caused by its good solubility in ethanol which made crystallization of this compound less efficient. The structures and purity of obtained compounds were confirmed by ^{1}H, ^{13}C, ^{11}B, and ^{19}F (when appropriate) NMR spectroscopy, elemental analysis and, in the case of **1**, single crystal X-ray measurements (for details see Supporting Information). Specifically, the ^{11}B NMR chemical shifts of **1-8**, and **9-10** are *ca.* 6-7 ppm, and 1-2 ppm, respectively, i.e., they fall in the range typical of tetrahedral boron atoms with C_2NO environment. These values are lower than those reported for related diarylborinic 8-oxyquinolinates (*ca.* 10 ppm).[2,26]

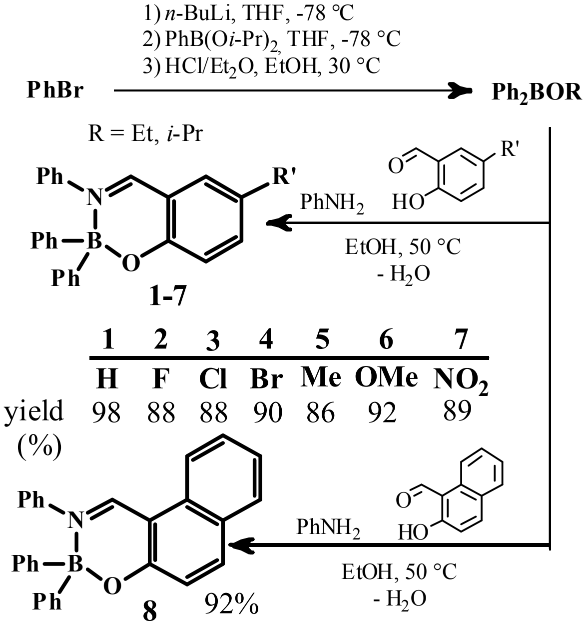

Scheme 1. Synthesis of **1-8** *via* multicomponent reaction.

We have observed that the ^{1}H NMR chemical shifts of aldimine protons (C**H**=N) in **1**–**7** (solvent: acetone-d_6) correlate strongly (R^2 = 0.95) with Hammett σ_p^- constants of R' substituents[34,35] attached to the salicydene fragment at the 6-position (**Figure 2**). The same signal correlates also with σ_p, σ_p^+ and σ_m, (**Figure S2** in Supporting Information) but with lower values of R^2 (0.91, 0.77 and 0.76, respectively). A stronger correlation with σ_p^- Hammett constants suggests that charge density on the aldimine hydrogen atom is modulated mainly by a resonance effect of a substituent at the 6-position on the oxygen atom, which in turn impacts the charge density distribution along the O-B-N=C pathway. It is worth noticing that ^{1}H NMR chemical shifts of aldimine protons in **9** and **10** are deshielded with respect to **1** by 0.11 and 0.34 ppm, respectively. This indicates that the impact of electron-withdrawing fluorinated phenyl groups on the charge density distribution is not limited to the boron atom but it spreads further across the entire chelate ring. A more detailed discussion of the correlation is given below in the section *Structure-properties correlation analysis*. It should be noted that correlations between ^{13}C NMR chemical shifts of **C**H=N carbon atoms and the Hammett constants were already investigated.[36]

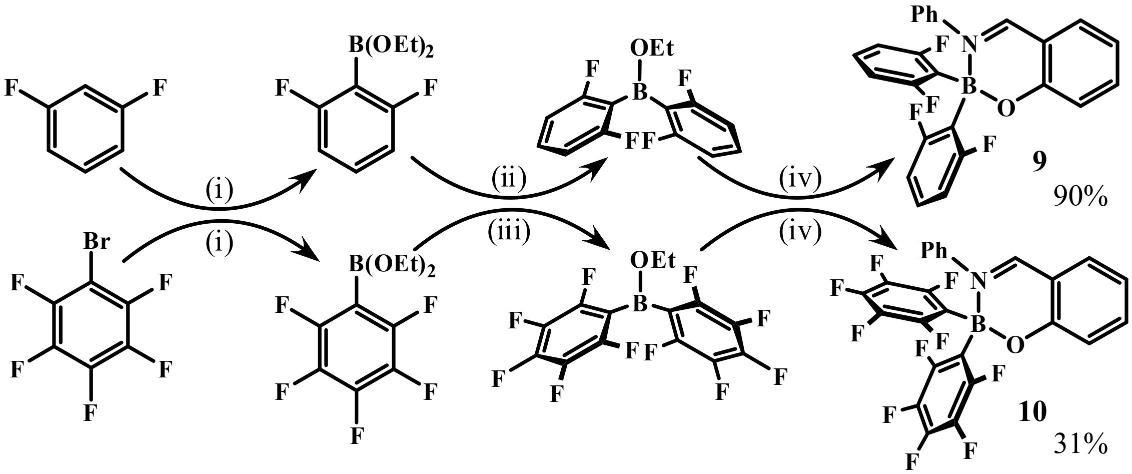

Scheme 2. The synthesis of compounds **9** and **10**. (i) 1) *n*-BuLi, 2) B(OEt)$_3$, 3) TMSCl or 2 M HCl/Et$_2$O; (ii) 1) 2,6-F$_2$C$_6$H$_3$Li, 2) TMSCl; (iii) 1) C$_6$F$_5$Li; 2) 2 M HCl/Et$_2$O; (iv) aniline, salicylaldehyde, EtOH.

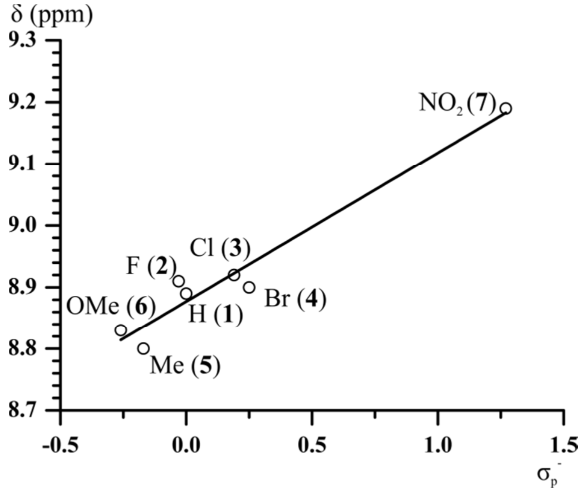

Figure 2. Chemical shifts of the C**H**=N hydrogen atoms for compounds **1**-**7** *versus* Hammett σ_p^- constants (R^2 = 0.95 and R(correlation) = 0.98; R^2 = 0.63 and R(correlation) = 0.80 after excluding **7**). Data were gathered for 0.1 M solutions in acetone-d$_6$ at 298 K.

Optical properties. UV-Vis absorption and emission spectra of **1-10** were recorded in CH_2Cl_2 under ambient conditions. Emission spectra were obtained after excitation at the longest wavelength absorption band. The results are summarized in **Table 1** and depicted in **Figure 3**. Absorption and emission maxima are observed in the range of 390-437 nm and 506-590 nm, respectively. Thus, it is clear that functionalization of the parent compound **1** is reflected by significant shifts of the spectral bands. Overall, compounds **5** and **6** carrying electron-donating functional groups (EDG = 6-Me and 6-OMe, respectively) feature a bathochromic shift with respect to **1**, whereas a reversed effect was observed for **7** possessing the electron-withdrawing 6-NO_2 substituent. The influence of the halogen atoms on the electron density distribution can be divided into a positive mesomeric and a negative inductive effect. We observed a combination of these effects in our previous report for systems with halogenated Q chromophores.[2] However, in this case it seems that the halogen mesomeric effect is more important for tuning the emission of compounds **2**-**4**. Compound **8** (bearing naphthalene-based chromophore) features a red-shifted absorption band with respect to **1** [λ_{abs} (**8**) = 427 *vs* λ_{abs} (**1**) = 400 nm] but its emission band remains unchanged.

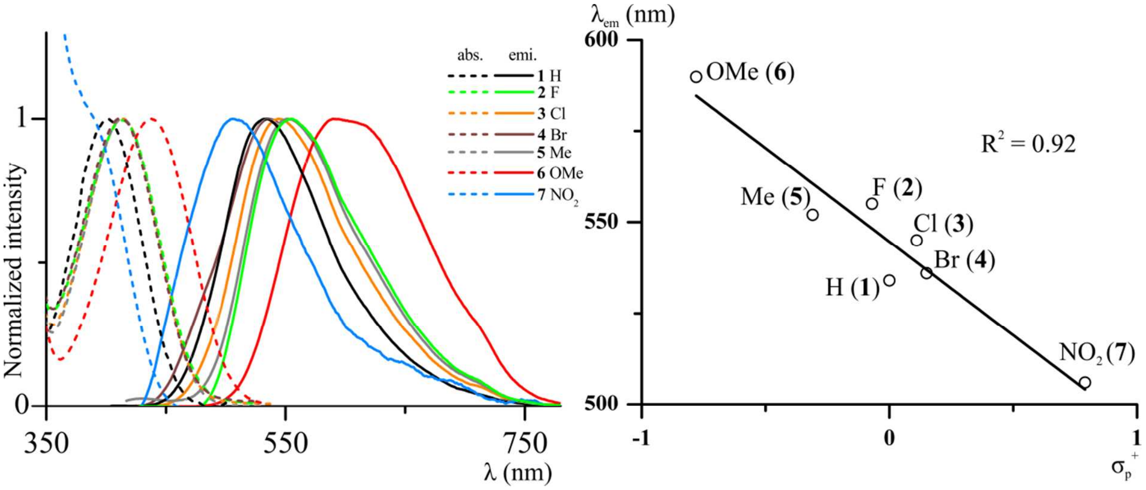

Figure 3a. Absorption and fluorescence spectra of **1**-**7** in CH_2Cl_2 (at rt) and plot of wavelengths of emission maxima for **1**-**7** *versus* Hammett σ_p^+ constants ($R^2 = 0.92$).

Interestingly, compounds **9** and **10** have their emission bands significantly blue-shifted with respect to **1** (by 20-25 nm) (**Figure 3b**). Such a strong effect of the fluorination of the phenyl groups attached to the boron atoms on λ_{em} was not observed for 8-oxyquinolinato diarylborinic Q complexes.[37,38] In contrast to the case of **1** and **10**, it was recently reported that the replacement of Ph_2B with $(C_6F_5)_2B$ moiety in diarylboron diketonates resulted in the increase of λ_{em} by *ca.* 20 nm.[39] The blue-shifted emission for **9-10** is consistent with significantly smaller Stokes shifts (Δ = 113-115 nm) with respect to **1** (Δ = 134 nm). This can be rationalized in terms of smaller conformational changes in the excited states of **9-10** compared to **1**. Thus, it seems that chelate rings in *boranils* are generally more susceptible to such changes than more rigid five-membered ones in borinic Q complexes. However, the use of more Lewis acidic boron centre (due to fluorination of aryl groups) apparently decreases the extent of structural reorganization upon excitation. A similar situation occurs for **7** where both the Stokes shift and λ_{em} are comparable to values found for **9-10**.

We have observed a linear correlation ($R^2 = 0.92$) between wavelength of emission for **1-7** and σ_p^+ Hammett constants (**Figure 3a**). Maxima of emission are moderately/weakly correlated with σ_p, σ_p^- and σ_m, (**Figure S5**) (with R^2 values of 0.75, 0.70 and 0.33, respectively). A possible rationalization of these correlations is discussed in the section *Structure-properties correlation analysis*. It should be noted that correlations between optical properties and the Hammett constants were already investigated for aluminium 8-oxyquinolinato complexes and other systems.[40–44]

Table 1. Experimental and calculated photophysical properties of **1-10**.

		Experimental					TD-DFT	
	Compound	λ_{max} [nm] [a,b]	ε [M^{-1} cm^{-1}]	λ_{em} [nm] [a]	Δ [nm]	Φ [%] [a,c]	λ_{max} [nm] [d]	λ_{em} [nm] [d]
1	**$[Ph]_2B$[6-H-Sal][Ani]**	400	4600	534	134	7	415 (0.072)	464 (0.0196)
2	**$[Ph]_2B$[6-F-Sal][Ani]**	413	4900	555	142	2	430 (0.076)	484 (0.020)
3	**$[Ph]_2B$[6-Cl-Sal][Ani]**	412	5300	545	133	7	430 (0.073)	481 (0.022)
4	**$[Ph]_2B$[6-Br-Sal][Ani]**	415	5400	536	121	4	432 (0.072)	481 (0.023)
5	**$[Ph]_2B$[6-Me-Sal][Ani]**	413	5100	552	139	17	424 (0.076)	744 (0.021)
6	**$[Ph]_2B$[6-OMe-Sal][Ani]**	437	5100	590	153	5	452 (0.087)	683 (0.041)
7	**$[Ph]_2B$[6-NO_2-Sal][Ani]**	390	6400	506	116	1	394 (0.062)	533 (0.017)
8	**$[Ph]_2B$[Naft-Sal][Ani]**	424	7600	534	110	4	420 (0.155)	480 (0.28)
9	**[2,6-diFPh]$_2$B[6-H-Sal][Ani]**	399	5700	514	115	17	407 (0.098)	475 (0.036)
10	**[pentaFPh]$_2$B[6-H-Sal][Ani]**	396	4800	509	113	12	400 (0.096)	–

[a] Measured in CH_2Cl_2. [b] $c = 5 \times 10^{-3}$ M. [c] Relative to Coumarine 153 in EtOH at room temperature. Excited at the longest wavelength absorption. [d] the value of oscillator strength (*f*) is given in parentheses. Calculations done with TD-RB3LYP/6-31+g(d,p) level of theory. Abbreviations: Ani – aniline moiety, Sal – salicydene moiety.

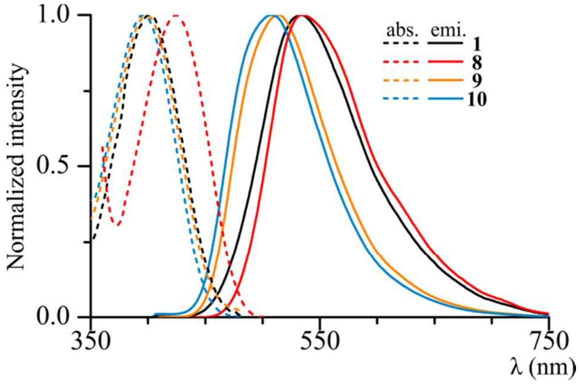

Figure 3b. Absorption and fluorescent spectra of **8-10** (and **1**, for comparison) in CH_2Cl_2.

Molecular orbital calculations. We have supported experimental results with theoretical calculations at the TD-RB3LYP/6-31+g(d,p) level of theory. Our computational studies were accomplished using B3LYP without the use of PCM model. It was proved that for such a combination (PCM-B3LYP) the correlation of theoretical results with experiment is worse than for the pure B3LYP potential.[45] We have established both the ground state geometry and first singlet excited state geometry which allowed for theoretical analysis of light absorption and emission. The final data are gathered in **Table 1** (and **Table S2**). Predicted absorption bands reproduce experimentally observed trends. However, the exact values differ substantially in some cases. Obtained systems undergo mainly HOMO→LUMO excitations with the exception of **7**, where deep HOMO−4/HOMO−3→LUMO excitations are observed. Clearly, the presence of functional groups at the 6-position affects the energies of the frontier orbitals (**Figure 4**). HOMO levels are located on salicydene fragments, whereas LUMOs have contributions from aniline rings.

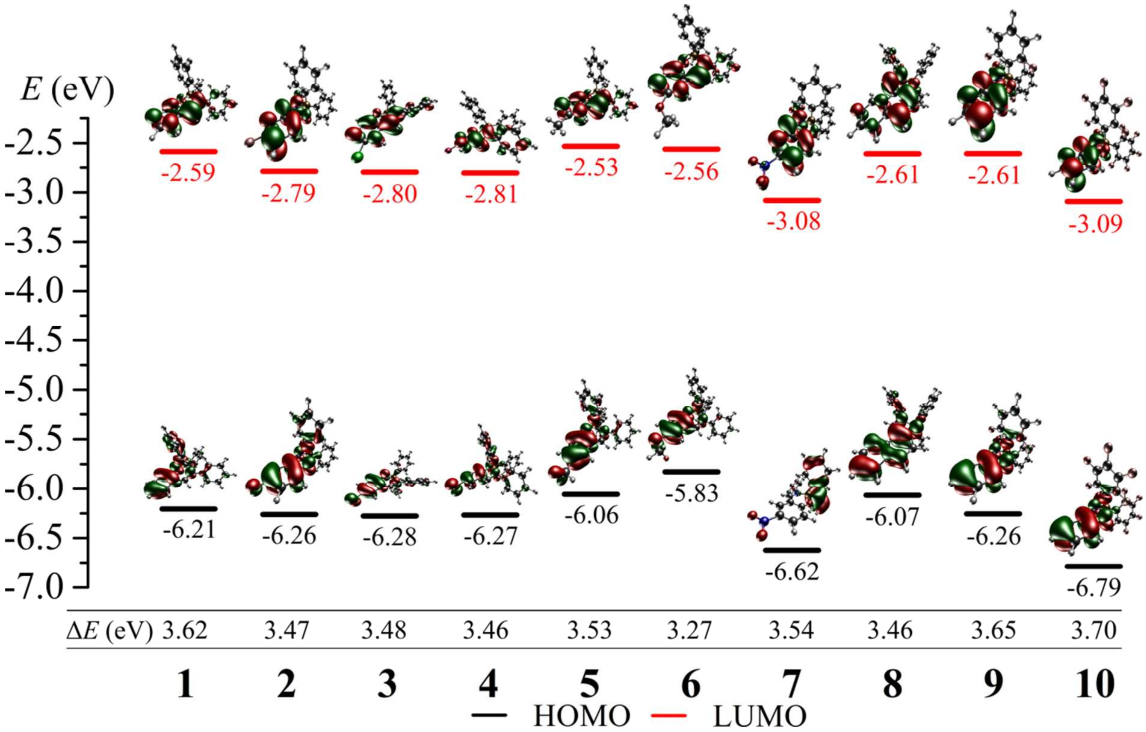

Figure 4. Plot of HOMO and LUMO orbitals (along with their energies, and energy gap) generated for systems **1-10** (isosurface 0.3 e Å^{-3}). Calculated at TD-RB3LYP/6-31+g(d,p) level of theory.

Structure-properties correlation analysis. The Hammett σ_p^+ constants were defined for a situation where a positive charge is generated at the reaction centre located at the *para* position of the aromatic ring with respect to a substituent. The correlation of λ_{em} with σ_p^+ constants may suggest that there is a positive charge on the salicylidene moiety due to charge transfer to phenyl group of aniline in the first excited singlet state. On the other hand, a good correlation of $\delta_{CH=N}$ with σ_p^- indicates that functional groups influence the charge density distribution in the chelate ring *via* strong resonance effect on the oxygen atom. In order to clarify this correlation, we have performed QTAIM analysis of the calculated charge density distributions for **1-7** (at B3LYP/6-31+g(d,p) levels of theory, QTAIM analysis was done with *AIMAll*[46] suit of programs). The obtained topological parameters and integrated atomic charges (**Tables S4-S10**) were checked against possible correlation with both the shifts of the ^{1}H NMR signals of the C**H**=N hydrogen ($\delta_{CH=N}$) atoms and the maxima of emission (λ_{em}). For established linear correlations ($y = a + bx$, y is either $\delta_{CH=N}$ or λ_{em}, and x are tested topological parameters) the R^2, and Δ_{rel}^{-1} factors were calculated (for results, see **Table S11-S12**). The Δ_{rel}^{-1} factor (given in %) is the reciprocal of the relative standard deviation. This way, the higher the Δ_{rel}^{-1}, the more meaningful the correlation. All correlations were checked with the

Snedecor's F-test at the 5% significance level and only the ones, which satisfy the test, are discussed. All statistical calculations were done in program *OriginPro*.[47] The numbering scheme used for discussion, along with R^2 coefficients obtained for correlation of $\delta_{CH=N}$ or λ_{em} with chosen topological parameters, is presented in **Figure 5**.

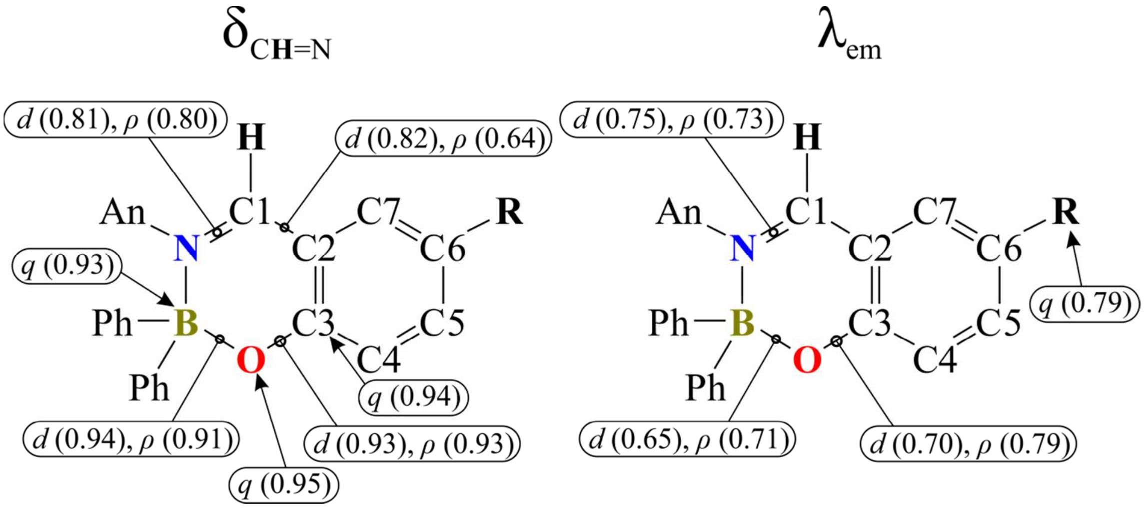

Figure 5. The numbering scheme along with R^2 coefficients obtained for correlation of $\delta_{CH=N}$ or λ_{em} with chosen topological parameters (*d* – interatomic distance (Å), *ρ* – charge density at the bond critical point ($e \cdot Å^{-3}$), *q* – is the integrated charge. In case of R, *q* is integrated for an atom attached to C(6) carbon, *e.g.*, for NO_2 group, the charge of the N atom was considered). All parameters were calculated for the optimised ground state geometries of **1**-**7**.

Considering correlations of the $\delta_{CH=N}$ with topological parameters (*d* and *ρ*), the equally high R^2 values were found for the O-C(3) bond which is at the *para* position with respect to the functional groups ($R^2 = 0.93$) as well as for the B-O bonds. This supports our previous conclusion concerning the correlation of the σ_p^- Hammett constants, that the charge density on the aldimine H atom is modulated mainly by the charge density distribution along the O-B-N=CH pathway. On the contrary, the parameters of C(1)-C(2) bond in the *meta* position with respect to the functional group at the 6-position are not so strongly correlated ($R^2 = 0.64$-0.82). It should be noticed that the ellipticities of the B-O and the B-N bonds are also correlated with $\delta_{CH=N}$ ($R^2 = 0.95$). Finally, integrated charges for the boron and the oxygen atoms and C(3) atoms are strongly correlated with $\delta_{CH=N}$ ($R^2 = 0.93$-0.95). The analyzed ^1H NMR chemical shifts correlate also with the topological parameters of the N-C(An) bonds (**Table S10**).

Finally, correlations of λ_{em} with topological parameters of C(3)-O and B-O bonds are weaker than those for $\delta_{CH=N}$ ($R^2 \approx 0.7$). We have searched for the correlation between the properties of the bond between C(6) atom and the atom from the R group attached directly to C(6) atom (*e.g.,* for NO_2 group we have analyzed the charges on the N atom). It seems that a relatively strong correlation is also observed for the integrated charges of those atoms (R^2 = 0.79).

Time-dependent optical and NMR measurements. We wanted to rationalize relatively low Φ values observed for described systems. For systems with NO_2 groups, such as **7** and borinic system analysed by Jäkle and co-workers,[12] Lakowicz stated that a non-radiative decay is more efficient than radiative relaxation which results in lowering of Φ.[48] The quenching character of other functional groups was not discussed in-depth. Initially, we have recorded time-dependent UV-Vis absorption (TDA) spectra of **1** in CH_2Cl_2 solution. Importantly, they revealed significant changes of the band intensities at 264, 348 and 400 nm (**Figure 6**).

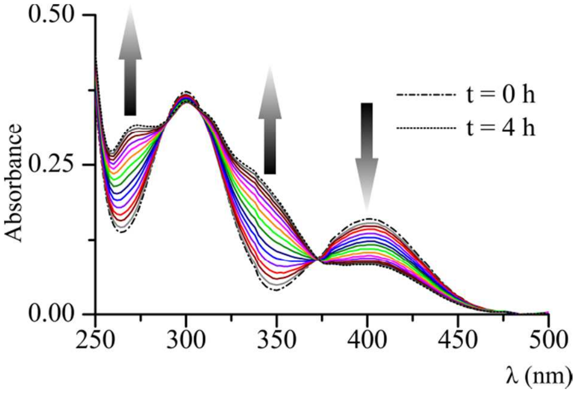

Figure 6. Time-dependent UV-Vis absorption spectra showing instability of **1** in CH_2Cl_2 solution (*T* = 298 K).

An overlay of the UV-Vis spectrum of **1** and salicydeneaniline points to a gradual decomposition of **1** in a dilute solution (**Figure S6**). This can be attributed to the breaking of the B-N and the B-O bonds of **1** upon interaction with traces of water, which is consistent with our previous findings concerning a labile character of the B-N bonds.[26,49] It is also in line with the elongation of the B-N bond in comparison with Q borinic complexes. It was observed that other (O,N)-boron chelate complexes, namely 2-(2'-hydroxyphenyl)benzoxazole difluoroborates are also prone to deboronation in alcohols and DMSO.[11] Measurements done for **2-7** directly after preparation of respective solutions and repeated after 1 hour revealed similar changes as the ones observed for the UV-Vis spectra of **1**. Unlike **1-7**, the TDA measurements for **8**, **9** and **10** revealed their higher stability (**Figure S7**). A partial decomposition of **1-7** in dilute solutions makes the obtained values of quantum yields of emission (and values of ε for light absorption) artificially low and, hence, less reliable even though measurements for all compounds were done shortly after preparation of solutions. Nevertheless, we present them for comparison with other published data. It should be stressed that the compounds were recovered after removal of the solvent from solutions prepared for UV-Vis measurements, which proved the reversible nature of observed processes. It is also possible that apart of reduced concentration of emitter, the fluorescence can be additionally decreased by other processes arising from *collisional* or *static* quenching, *e.g.*, arising from interactions of emitter molecules with products of decomposition of *boranils*.

Our studies were supported by TD ^{1}H and ^{11}B NMR measurements for **1** (**Figure S9**). In the ^{11}B NMR spectra, a distinct signal of three-coordinate borinic species (at *ca*. 45 ppm)[50] was observed whereas a signal of the CHO group appeared in the ^{1}H NMR spectrum (at *ca*. 11 ppm) indicating some degradation of a salicylaldimine ligand. These results correspond with obtained TD-UV-Vis spectra. Judging from the different time scales of the UV-Vis and the NMR experiments, highly diluted UV-Vis samples are much more vulnerable to decomposition than more concentrated samples for NMR as the intensity of the longest wavelength UV-Vis absorption band significantly decreases. Presumably, when the concentration of **1** is low, then the molar ratio of water impurity and **1** is relatively high, which means that hydrolytic cleavage of **1** may occur to a significant extent. Obviously, for more concentrated samples used for NMR studies, the ratio of H_2O to **1** is low, which means that only a small amount of the complex may undergo a slow degradation.

Conclusions

In conclusion, an improved one-pot method for the preparation of a series of functionalized diarylborinic salicydeneaniline complexes has been developed. The isolation of their borinic acid precursors is not required and they can be treated *in situ* with respective salicylaldehydes and aniline to give final products. Thus, there is also no need for the separate synthesis of a salicydeneaniline ligand. It was demonstrated that optical properties of obtained systems in CH_2Cl_2 solution can be tuned by a proper functionalization of salicydene moiety at the 6-position. Specifically, there is a distinct dependence of the positions of emission bands on the electronic character of the substituent. The obtained ^{1}H NMR chemical shifts of the C**H**=N protons ($\delta_{C\mathbf{H}=N}$) and maxima of emission (λ_{em}) correlate with the Hammett σ_p^- and σ_p^+ constants, respectively. This study was expanded by the correlation analysis of $\delta_{C\mathbf{H}=N}$ and λ_{em} with topological parameters of the charge density distribution. We believe that knowledge about existence of such correlations may be helpful for a rational design of materials with desirable colour of emission.

It should be stressed that *boranils* **1-7** tend to undergo reversible hydrolytic deboronation upon reaction with trace amounts of water present in or absorbed by the solvent during time-dependent UV-Vis absorption spectral studies. However, we have found that the stability of such systems can be improved either by using strongly electron withdrawing ligands attached directly to the boron atom or by using a naphthalene-based salicydeneaniline counterpart. In the former case, this can be rationalized by the fact that electron-withdrawing ligands increase the Lewis acidity of the boron atom, which in turn increases the strength of B-O and B-N bonds. This work has demonstrated that the matter of stability of *boranils*, specifically when used at low concentrations under ambient conditions, should be taken into account in future developments.

Experimental Section

General comments. All used reagents were provided by Aldrich Chemical Company. *n*-BuLi was used as a concentrated solution (10 M) in hexane. Solvents (THF and Et_2O) used for reactions were dried by heating to reflux with sodium/benzophenone and distilled under argon. Ethanol (96%) denatured with Et_2O was used. Reactions and manipulations involving air and moisture-sensitive reagents were carried out under argon atmosphere.

NMR spectroscopy characterization. ^{1}H, ^{19}F and ^{13}C NMR spectra were recorded on a Varian Mercury 400 MHz spectrometer. The ^{11}B NMR spectra were recorded on Bruker Avance III NMR 300 MHz spectrometer. Chemical shifts of the ^{1}H and ^{13}C NMR spectra were referenced to TMS by using known chemical shifts of solvent residual peaks. In the ^{13}C NMR spectra of diarylborinic complexes, the resonances of boron-bound carbon atoms were not observed in most cases as a result of their broadening by a quadrupolar boron nucleus. ^{11}B and ^{19}F NMR spectra were referenced to $BF_3 \cdot Et_2O$ and $CFCl_3$, respectively. ^{1}H and ^{13}C NMR resonances for **1-7**, **9-10,** and **8** were assigned according to **Scheme 3** and **4**, respectively.

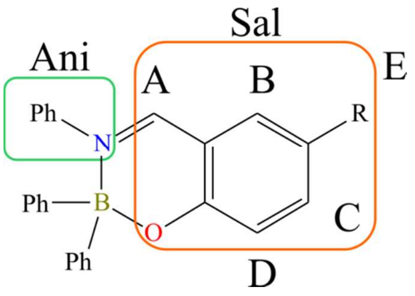

Scheme 3. The assignment scheme of ^{1}H NMR resonances (R is the functional group) for **1-7** and **9-10.**

Synthesis of diisopropyl phenylboronate. Bromobenzene (31.4 g, 0.20 mol) was added dropwise to a stirred solution of *n*-BuLi (21.0 mL, 0.21 mol) in THF (100 mL) at −78 °C. After *ca*. 30 min, triisopropyl borate (49.0 mL, 0.21 mol) was added dropwise. The mixture was stirred at −78 °C for 30 min. Then it was warmed to 30 °C and quenched with a solution of 2 M HCl in Et_2O (125 mL, 0.25 mol). Solvents were removed and the residue was subjected to fractional vacuum distillation to give the product as a colourless liquid, b.p. 70-79 °C (2 Tr). Yield 38.62 g (94 %). ^{1}**H NMR** (400 MHz, acetone-d$_6$): δ = 7.41-7.29 (m, 3H, **Ph**), 7.59-7.52 (m, 2H, **Ph**), 4.62 (sept, J_{HH} = 6.1 Hz, 2H, C**H**), 1.21 (d, J_{HH} = 6.1 Hz, 12H, C**H$_3$**) ppm. ^{11}**B NMR** (64 MHz, Acetone-d$_6$): δ = 28 ($w_{1/2}$ = 130 Hz) ppm.

Synthesis of [Ph]$_2$B[6-H-Sal][Ani] (1). Bromobenzene (1.57 g, 10.0 mmol) was added dropwise to a stirred solution of *n*-BuLi (1.02 mL, 10.0 mmol) in THF (30 mL) at −78 °C. After 30 min diisopropyl phenylboronate (2.06 g, 10.0 mmol) was added dropwise. Subsequently the mixture was stirred for *ca.* 30 min and then allowed to reach the room temperature. The solvent was removed under vacuum and the residue was dissolved in EtOH (25 mL). The solution was treated with 2 M HCl in Et_2O (5.0 mL, 10.0 mmol) at 40 °C. After 20 min the mixture was warmed to 50 °C and then aniline (1.21 g, 13.0 mmol) and salicylaldehyde (1.10 g, 9.0 mmol) were simultaneously added resulting in a yellow coloration of the mixture. It was concentrated under vacuum and cooled to 0 °C. The crude product was filtered. The solid was washed with cold ethanol and hexane, and dried under vacuum to give a yellow crystalline material. Yield 3.19 g (8.8 mmol, 98 %). M.p. 151-153 °C, from DSC: 156.8 °C. ^{1}**H NMR** (400 MHz, $CDCl_3$): δ = 8.35 (s, 1H, **A**), 7.57-7.39 (m, 5H, **Ar, Ani**), 7.32 (dd, J_{HH} = 7.8, J_{HH} = 1.6 Hz, 1H, **B**), 7.27-7.13 (m, 9H, **Ar**), 7.03 (dd, J_{HH} = 8.2, J_{HH} = 1.6 Hz, 3H, **Ar**), 6.82 (dt, J_{HH} = 7.5, J_{HH} = 0.8 Hz, 1H, **E**) ppm. ^{1}**H NMR** (400 MHz, acetone-d$_6$): δ = 8.89 (s, 1H, **A**), 7.60 (dd, J_{HH} = 7.8, J_{HH} = 1.7 Hz, 1H), 7.50 (ddd, J = 8.5, J_{HH} = 7.2, J_{HH} = 1.8 Hz, 1H), 7.40 (dd, J_{HH} = 7.9, 1.6 Hz, 4H), 7.27-7.16 (m, 5H), 7.14-7.03 (m, 6H), 6.91-6.81 (m, 2H). ^{13}**C{^{1}H} NMR** (100.6 MHz, $CDCl_3$): δ = 162.8 (N=**C**H), 162.3 (**Sal**, O-**C**), 145.4 (**Ani**, N-**C**), 138.7, 133.6, 132.1, 128.6, 128.2, 126.9, 126.3, 124.4, 120.1, 118.8, 118.1 ppm. ^{11}**B NMR** (64 MHz, acetone-d$_6$): δ = 6 ($w_{1/2}$ = 192 Hz) ppm. Anal. Calcd for $C_{25}H_{20}BNO$ (361.24): C 83.21, H 5.58, N 3.88%, found C 83.12, H 5.57, N 3.97%. UV-Vis: λ_{max} = 400 nm, ε = 4600 $M^{-1}cm^{-1}$. Fluorescence: λ_{exc} = 400 nm, λ_{em} = 534 nm, Φ = 7%.

Compounds **2-8** were prepared as described for **1**.

Synthesis of [Ph]$_2$B[6-F-Sal][Ani] (2). Starting materials: THF (20 mL), bromobenzene (0.93 g, 6.0 mmol), *n*-BuLi (0.65 mL, 6.5 mmol), diisopropyl phenylboronate (1.23 g, 6.0 mmol), EtOH (10 mL), 2 M HCl in Et$_2$O (3.25 mL, 6.5 mmol), aniline (0.57 g, 6.0 mmol), 5-fluoro-2-hydroxybenzaldehyde (0.77 g, 5.5 mmol). 1.81 g (4.7 mmol, 88%). M.p. 136-138 °C. **^{1}H NMR** (400 MHz, acetone-d$_6$): δ = 8.91 (s, 1H, **A**), 7.43-7.36 (m, 5H), 7.31 (ddd, J_{HH} = 9.1, 3.2 Hz, J_{HF} = 8.3 Hz, 1H, **C**), 7.27-7.18 (m, 5H), 7.15-7.04 (m, 6H), 6.91 (dd, J_{HH} = 9.1 Hz, J_{HF} = 4.3 Hz, 1H, **D**) ppm. **^{11}B NMR** (96 MHz, acetone-d$_6$) δ = 6 ($w_{1/2}$ = 170 Hz) ppm. **^{13}C{^{1}H} NMR** (100.6 MHz, acetone-d$_6$) δ = 164.8 (s, N=CH), 159.5 (d, J_{CF} = 269 Hz, **Sal**, C-F), 154.5 (**Sal**, O-**C**), 146.3 (**Ani**, N-**C**), 134.4, 129.3, 129.0, 127.4, 126.5 (d, J_{CF} = 24 Hz, **Sal**), 126.4, 125.3, 121.7 (d, J_{CF} = 8 Hz, **Sal**), 119.3 (d, J_{CF} = 9 Hz, **Sal**), 117.6 (d, J_{CF} = 24 Hz, **Sal**) ppm. Anal. Calcd for $C_{25}H_{19}BFNO$ (379.23): C 79.18%; H 5.05%; N 3.69%, found C 79.07%, H 5.24%, N 3.86%. UV-Vis: λ_{max} = 413 nm, ε = 4900 $M^{-1}cm^{-1}$. Fluorescence: λ_{exc} = 413 nm, λ_{em} = 555 nm, Φ = 2%.

Synthesis of [Ph]$_2$B[6-Cl-Sal][Ani] (3). Starting materials: THF (30 mL), bromobenzene (1.57 g, 10.0 mmol), *n*-BuLi (1.02 mL, 10.0 mmol), diisopropyl phenylboronate (2.06 g, 10.0 mmol), EtOH (25 mL), 2 M HCl in Et$_2$O (5.0 mL, 10.0 mmol), aniline (1.21 g, 13.0 mmol), 5-chloro-2-hydroxybenzaldehyde (1.41 g, 9.0 mmol). Yield: 3.14 g (7.9 mmol, 88%). M.p. 127-128 °C, from DSC 129.2 °C. **^{1}H NMR** (400 MHz, acetone-d$_6$): δ = 8.92 (s, 1H, **A**), 7.65 (d, J_{HH} = 2.7 Hz, 1H, **B**), 7.48 (dd, J_{HH} = 8.9, J_{HH} = 2.7 Hz, 1H, **C**), 7.39 (dd, J_{HH} = 7.8, J_{HH} = 1.6 Hz, 4H, **Ar**), 7.29-7.17 (m, 5H, **Ar**), 7.16-7.04 (m, 6H, **Ar**), 6.91 (d, J_{HH} = 8.9 Hz, 1H, **D**) ppm. **^{13}C{^{1}H} NMR** (100.6 MHz, acetone-d$_6$): δ = 164.9 (N=**C**H), 161.7 (**Sal**, O-**C**), 146.3 (**Ani**, N-**C**), 138.6, 134.5, 132.4, 129.4, 129.1, 127.5, 127.0, 125.4, 123.4, 122.1, 120.5 ppm. **^{11}B NMR** (64 MHz, acetone-d$_6$): δ = 6 ($w_{1/2}$ = 256 Hz) ppm. Anal. Calcd for $C_{25}H_{19}BClNO$ (395.69): C 75.88, H 4.84, N 3.54, Cl 8.96%, found C 75.70, H 4.87, N 3.66, Cl 9.08%. **UV-Vis**: λ_{max} = 412 nm, ε = 5300 $M^{-1}cm^{-1}$. Fluorescence: λ_{exc} = 412 nm, λ_{em} = 545 nm, Φ = 7%.

Synthesis of [Ph]$_2$B[6-Br-Sal][Ani] (4). Starting materials: THF (30 mL), bromobenzene (1.57 g, 10.0 mmol), *n*-BuLi (1.02 mL, 10.0 mmol), diisopropyl phenylboronate (2.06 g, 10.0 mmol), EtOH (25 mL), 2 M HCl in Et$_2$O (5.0 mL, 10.0 mmol), aniline (1.21 g, 13.0 mmol), 5-bromo-2-hydroxybenzaldehyde (1.81 g, 9.0 mmol). Yield 3.55 g (8.1 mmol, 90%). M.p. 137-138 °C, from DSC 142.0 °C. **^{1}H NMR** (400 MHz, $CDCl_3$): δ = 8.30 (s, 1H, **A**), 7.51 (d, J_{HH} = 8.8 Hz, 1H, **C**), 7.45-7.38 (m, 5H, **Ani**), 7.26-7.15 (m, 9H, **Ar**), 7.03 (s, 1H, **Ar**), 7.01 (s, 1H, **Ar**), 6.92 (d, J_{HH} = 8.8 Hz, 1H, **D**) ppm**.** ^{1}**H NMR** (400 MHz, acetone-d$_6$): δ = 8.90 (s, 1H, **A**), 7.77 (d, J = 2.6 Hz, 1H, **B**), 7.58 (dd, J = 8.9, 2.6 Hz, 1H, **D**), 7.42 – 7.36 (m, 4H, **Ar**), 7.28 – 7.17 (m, 5H, **Ar**), 7.16 – 7.03 (m, 6H, **Ar**), 6.86 (d, J = 8.9 Hz, 1H, **C**). ^{13}**C{^{1}H} NMR** (100.6 MHz, acetone-d$_6$): δ = 164.6 (N=CH), 161.9 (**Sal**, O-**C**), 146.2 (**Ani**, N-**C**), 141.3, 135.4, 134.4, 129.3, 129.0, 127.4, 126.9, 125.3, 122.4, 121.2, 120.1, 110.1 (**C**-Br) ppm. ^{11}**B NMR** (64 MHz, DMSO-d$_6$): δ = 6 (w$_{1/2}$ = 1280 Hz) ppm. Anal. Calcd for $C_{25}H_{19}BBrNO$ (440.14): C 68.22, H 4.35, N 6.91. Br 18.15%, found C 68.01, H 4.50, N 3.31, Br 18.18%. UV-Vis: λ_{max} = 415 nm, ε = 5400 M^{-1}cm^{-1}. Fluorescence: λ_{exc} = 415 nm, λ_{em} = 536 nm, Φ = 4%.

Synthesis of [Ph]$_2$B[6-Me-Sal][Ani] (5). Starting materials: THF (30 mL), bromobenzene (1.57 g, 10.0 mmol), *n*-BuLi (1.02 mL, 10.0 mmol), diisopropyl phenylboronate (2.06 g, 10.0 mmol), EtOH (25 mL), 2 M HCl in Et$_2$O (5.0 mL, 10.0 mmol), aniline (1.21 g, 13.0 mmol), 5-methyl-2-hydroxybenzaldehyde (1.23 g, 9.0 mmol). Yield 2.91 g (7.8 mmol, 86%). M.p. 143-146 °C, from DSC 145.3 °C. ^{1}**H NMR** (400 MHz, acetone-d$_6$): δ = 8.80 (d, J_{HH} = 0.6 Hz, 1H, **A**), 7.40-7.37 (m, 5H, **Ani**), 7.33 (ddd, J_{HH} = 8.4 Hz, J_{HH} = 2.3 Hz, J_{HH} = 0.6 Hz, 1H, **C**), 7.26-7.15 (m, 5H, **Ar**), 7.14-7.02 (m, 6H, **Ar**), 6.79 (d, J_{HH} = 8.4 Hz, 1H, **D**), 2.21 (s, 3H, C**H$_3$**) ppm. ^{13}**C{^{1}H} NMR** (100.6 MHz, acetone-d$_6$): δ = 165.2 (N=**C**H), 161.1 (**Sal**, O-**C**), 146.5 (**Ani**, N-**C**), 140.4, 135.5, 134.4, 133.0, 129.2, 128.7, 128.5, 127.3, 126.7, 125.3, 119.9, 119.5, 20.1 (**C**H$_3$) ppm. ^{11}**B NMR** (64 MHz, acetone-d$_6$): δ = 6 (w$_{1/2}$ = 256 Hz) ppm. Anal. Calcd for $C_{26}H_{22}BNO$ (375.27): C 83.21, H 5.91, N 3.73%, found C 83.14, H 5.90, N 3.84%. **UV-Vis**: λ_{max} = 413 nm, ε = 5100 M^{-1}cm^{-1}. Fluorescence: λ_{exc} = 413 nm, λ_{em} = 552 nm, Φ = 17%.

Synthesis of [Ph]$_2$B[6-OMe-Sal][Ani] (6). Starting materials: THF (30 mL), bromobenzene (1.57 g, 10.0 mmol), *n*-BuLi (1.02 mL, 10.0 mmol), diisopropyl phenylboronate (2.06 g, 10.0 mmol), EtOH (40 mL), 2 M HCl in Et$_2$O (5.0 mL, 10.0 mmol), aniline (1.21 g, 13.0 mmol), 5-methoxy-2-hydroxybenzaldehyde (1.12 mL, 9.0 mmol). Yield 3.23 g (8.3 mmol, 92%). M.p. 168-169 °C, from DSC 173.9 °C (first cycle) and 173.6 °C (second cycle). ^{1}**H NMR** (400 MHz, CDCl$_3$): δ = 8.32 (s, 1H, **A**), 7.45-7.43 (m, 4H, **Ar**), 7.25-7.14 (m, 9H, **Ar**), 7.12 (dd, J_{HH} = 9.1, J_{HH} = 3.1 Hz, 1H, **C**), 7.05 (dd, J_{HH} = 8.0, J_{HH} = 1.5 Hz, 2H, **Ar**), 6.98 (d, J_{HH} = 9.1 Hz, 1H, **D**), 6.74 (d, J_{HH} = 3.1 Hz, 1H, **B**), 3.75 (s, 3H, -OC**H**$_3$) ppm. ^{1}**H NMR** (400 MHz, acetone-d$_6$): δ = 8.83 (s, 1H, **A**), 7.42-7.37 (m, 4H, **Ar**), 7.25-7.17 (m, 5H, **Ar**), 7.14-7.02 (m, 8H, **Ar**), 6.84 (d, J_{HH} = 8.8 Hz, 1H, **Ar**), 3.73 (s, 3H, **-OCH$_3$**). ^{13}**C{^{1}H} NMR** (100.6 MHz, acetone-d$_6$): δ = 164.9 (N=**C**H), 157.8 (**Sal**, O-**C**), 152.8 (**Sal**, MeO-**C**), 146.5 (**Ani**, N-**C**), 134.4, 129.2, 128.7, 128.1, 127.3, 126.7, 125.3, 121.1, 119.2, 114.2, 56.0 (O-**C**H_3) ppm. **^{11}B NMR** (64 MHz, acetone-d_6): $\delta = 6$ ($w_{1/2} = 190$ Hz) ppm. Anal. Calcd for $C_{26}H_{22}BNO_2$ (391.27): C 79.81, H 5.67, N 3.58%, found C 79.73, H 5.68, N 3.68%. UV-Vis: $\lambda_{max} = 437$ nm, $\varepsilon = 5100$ $M^{-1}cm^{-1}$. Fluorescence: $\lambda_{exc} = 437$ nm, $\lambda_{em} = 590$ nm, $\Phi = 5\%$.

Synthesis of [Ph]$_2$B[6-NO$_2$-Sal][Ani] (7). Starting materials: THF (30 mL), bromobenzene (1.57 g, 10.0 mmol), *n*-BuLi (1.02 mL, 10.0 mmol), diisopropyl phenylboronate (2.06 g, 10.0 mmol), EtOH (40 mL), 2 M HCl in Et_2O (5.0 mL, 10.0 mmol), aniline (1.21 g, 13.0 mmol), 5-nitro-2-hydroxybenzaldehyde (1.50 g, 9.0 mmol). A crude product was recrystallized from Et_2O. Yield 3.43 g (8.4 mmol, 89%). M.p. from DSC 167.8 °C. **^{1}H NMR** (400 MHz, acetone-d_6): $\delta = 9.19$ (s, 1H, **A**), 8.65 (d, $J_{HH} = 2.8$ Hz, 1H, **B**), 8.33 (dd, $J_{HH} = 9.0$, $J_{HH} = 2.8$ Hz, 1H, **C**), 7.42-7.40 (m, 4H, **Ar**), 7.30-7.22 (m, 5H, **Ar**), 7.18-7.10 (m, 6H, **Ar**), 8.65 (d, $J_{HH} = 9.0$ Hz, 1H, **D**) ppm. **^{13}C{^{1}H} NMR** (100.6 MHz, acetone-d_6): $\delta =$ 167.5 (N=**C**H), 165.7 (**Sal**, O-**C**), 146.2 (**Ani**, N-**C**), 140.5, 134.5, 133.4, 129.7, 127.8, 127.5, 125.6, 122.5, 121.2, 118.5. **^{11}B NMR** (64 MHz, acetone-d_6): $\delta = 7$ ($w_{1/2} = 256$ Hz) ppm. Anal. Calcd for $C_{25}H_{19}BN_2O_3$ (406.24): C 73.91, H 4.71, N 6.90%, found C 73.57, H 4.82, N 6.89 %. UV-Vis: $\lambda_{max} = 390$ nm, $\varepsilon = 6400$ $M^{-1}cm^{-1}$. Fluorescence: $\lambda_{exc} = 390$ nm, $\lambda_{em} = 506$ nm, $\Phi = 1\%$.

Synthesis of [Ph]$_2$B[Naft-Sal][Ani] (8). Starting materials: THF (30 mL), bromobenzene (1.57 g, 10.0 mmol), *n*-BuLi (1.02 mL, 10.0 mmol), diisopropyl phenylboronate (2.06 g, 10.0 mmol), EtOH (40 mL), 2 M HCl in Et_2O (5.0 mL, 10.0 mmol), aniline (1.21 g, 13.0 mmol), 2-hydroxynaphthalene-1-aldehyde (1.72 g). Yield 3.78 g (92%). M.p. 210-211 °C, from DSC 217.4 °C. **^{1}H NMR** (400 MHz, acetone-d_6): $\delta = 9.43$ (s, 1H, **A**), 8.34 (dd, $J_{HH} = 8.4$, $J_{HH} = 1.1$ Hz, $J_{HH} = 0.6$ Hz, 1H, **E**), 8.06 (d, $J_{HH} = 9.0$ Hz, 1H, **G**), 7.81 (ddd, $J_{HH} = 8.0$, $J_{HH} = 1.4$ Hz, $J_{HH} = 0.6$ Hz, 1H, **B**), 7.56 (ddd, $J_{HH} = 8.4$, $J_{HH} = 7.0$, $J_{HH} = 1.4$ Hz, 1H, **D**), 7.46-7.42 (m, 4H, **Ar**), 7.38 (ddd, $J_{HH} = 8.0$, $J_{HH} = 7.0$, $J_{HH} = 1.1$ Hz, 1H, **C**), 7.35-7.31 (m, 2H, **Ar**), 7.28-7.20 (m, 3H, **Ar**), 7.12 (d, $J_{HH} = 9.0$ Hz, 1H, **F**), 7.12-7.00 (m, 6H, **Ar**) ppm. **^{13}C{^{1}H} NMR** (100.6 MHz, acetone-d_6): $\delta = 165.1$ (N=**C**H), 160.0 (**sal**, O-**C**),146.9 (**Ani**, N-**C**), 140.6, 134.5, 133.4, 129.9, 129.6, 129.2, 128.4, 128.3, 127.3, 126.7, 125.6, 124.9, 121.7, 121.2, 112.7 ppm. **^{11}B NMR** (64 MHz, acetone-d_6): $\delta = 6$ ($w_{1/2} = 256$ Hz) ppm. Anal. Calcd for $C_{29}H_{22}BNO$ (411.30): C 84.86, H 5.39, N 3.41%, found C 84.88, H 5.35, N 3.49%. UV-Vis: $\lambda_{max} = 424$ nm, $\varepsilon = 7600$ $M^{-1}cm^{-1}$. Fluorescence: $\lambda_{exc} = 424$ nm, $\lambda_{em} = 534$ nm, $\Phi = 4\%$.

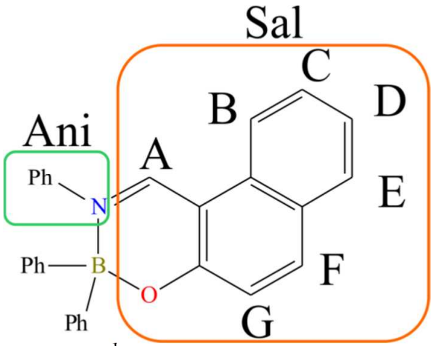

Scheme 4. The assignment scheme of ^{1}H NMR resonances for **8**.

Synthesis of 2,6-difluorophenylboronic diethyl ester. 1,3-Difluorobenzene (11.4 g, 0.10 mol) was added dropwise to a stirred solution of *n*-BuLi (10.2 mL, 0.102 mol) in THF (100 mL) at −78 °C. After *ca.* 20 min, triethyl borate (17.0 mL, 0.10 mol) was added dropwise. The mixture was stirred at −78 °C for 30 min, and afterwards warmed to -5 °C. Trimethylsilyl chloride (13.0 mL, 0.102 mol) was added, and the mixture was warmed to 30 °C. Solvents were removed and the residue was subjected to fractional vacuum distillation to give the product as a colourless liquid, b.p. 40-50 °C (2 Tr). Yield 18.39 g (86 %). ^{1}**H NMR** (400 MHz, $CDCl_3$): δ = 7.35-7.24 (m, 1H), 6.88-6.81 (m, 2H), 3.97 (q, J = 7.1 Hz, 4H. -OC**H**$_2$-), 1.24 (t, J = 7.1 Hz, 6H, -C**H**$_3$) ppm. ^{11}**B NMR** (64 MHz, $CDCl_3$): δ = 29 ($w_{1/2}$ = 120 Hz) ppm. ^{19}**F NMR** (376 MHz, $CDCl_3$): δ = −103.22 (t, J_{HF} = 6.5 Hz) ppm.

Synthesis of [2,6-diFPh]$_2$B[6-H-Sal][Ani] (9). 1,3-Difluorobenzene (0.23 g, 2.0 mmol) was added dropwise to a stirred solution of 10 M *n*-BuLi (0.2 mL, 2.0 mmol) in THF (5 mL) at −78 °C. After *ca.* 15 min, diethyl (2,6-difluorophenyl)boronate (0.43 g, 2.0 mmol) in THF (5 mL) was added dropwise. The mixture was stirred at −78 °C for 20 min. Then it was treated with a solution of 2 M HCl in Et_2O (1.1 mL, 2.2 mmol), and slowly warmed up to the room temperature. Aniline (0.20 g, 2.1 mmol) and salicylaldehyde (0.26 g, 2.1 mmol) in ethanol (5 mL) were added to a stirred solution at rt. The mixture was warmed to 50 °C. After *ca.* 1 hr the mixture was cooled to rt and concentrated in vacuo to give a yellow solid. A crude product was obtained by filtration of a cooled solution (*ca.* −30 °C) and washed with a cooled mixture of Et_2O and hexane. Then it was recrystallized from ethanol and dried under vacuum. Yield 0.76 g (1.8 mmol, *ca.* 90%). M.p. 210-212 °C. ^{1}**H NMR** (300 MHz, acetone-d$_6$): δ = 9.00 (s, 1H, N=C**H**), 7.71 (dd, J_{HF} = 7.7, 1.7 Hz, 1H, **Ani**), 7.59-7.44 (m, 3H, Ar), 7.38-7.21 (m, 3H, Ar), 7.13 (tt, J = 8.4, 6.5 Hz, 2H, Ph), 6.92 (ddd, J = 7.8, 7.2, 1.0 Hz, 1H, **Ph**), 6.84 (ddt, J = 8.4, 1.0, 0.6 Hz, **Ph**), 6.71-6.58 (m, 4H, Ar) ppm. ^{11}**B NMR** (96 MHz, acetone-d$_6$): δ = 2 ($w_{1/2}$ = 120 Hz) ppm. ^{13}**C NMR** (100.6 MHz, acetone-d$_6$): δ = 166.2 (dd, J_{CF} = 243, 15 Hz, **C**-F), 164.3 (s, 1H, N=CH), 161.1 (**Sal**, O-**C**), 144.8 (**Ani**, N-**C**), 138.8, 133.3, 129.2 (t, J_{CF} = 12 Hz, **Ph**), 128.6, 128.4, 123.4, 119.2, 119.1, 118.4, 110.6, 110.5, 110.3 ppm. ^{19}**F NMR** (376 MHz, acetone-d$_6$): δ = −103.78 (t, J_{HF} = 6.8 Hz) ppm. Anal. Calcd for $C_{25}H_{16}BF_4NO$ (433.21): C 69.31, H 3.72, N 3.23, F 17.54, found C 69.30, H 3.84, N 3.40%. UV-Vis: λ_{max} = 424 nm, ε = 7600 M^{-1}cm^{-1}. Fluorescence: λ_{exc} = 424 nm, λ_{em} = 534 nm, Φ = 4%.

Synthesis of Diethyl pentafluorophenylboronate. Pentafluorobromobenzene (12.4 g, 50 mmol) was added dropwise to a stirred solution of *n*-BuLi (5.6 mL, 56 mmol) in Et_2O (50 mL) at −78 °C. After *ca.* 15 min, triethyl borate (8.6 g, 50 mmol) was added dropwise. The mixture was stirred in −78 °C for 30 min, and then treated with solution of 2 M HCl in Et_2O (26 mL, 53 mmol). Then it was slowly warmed up to rt and pH was adjusted to *ca.* 2 by addition of *ca.* 1 mL of 2 M HCl in Et_2O and stirred overnight. After filtration, solvents were removed under reduced pressure and the residue was subjected to fractional vacuum distillation to give the product as a colourless liquid, b.p. 65-80 °C (2 Tr).Yield 11.4 g (86 %). ^{1}**H NMR** (400 MHz, $CDCl_3$): δ = 3.98 (q, J_{HH} = 7.1 Hz, 4H, CH_2), 1.24 (t, J_{HH} = 7.1 Hz, 6H, CH_3) ppm. ^{11}**B NMR** (128 MHz, $CDCl_3$): δ = 26 ($w_{1/2}$ = 128 Hz) ppm. ^{19}**F NMR** (376 MHz, $CDCl_3$): δ = −132.28 ÷ −132.63 (m, 2F), −153.45 (tt, J_{FF} = 19.8, 2.1 Hz, 1F), −161.82 ÷ −162.15 (m, 2F) ppm.

Synthesis of [pentaFPh]$_2$B[6-H-Sal][Ani] (10). Pentafluorobromobenzene (1.24 g, 5.0 mmol) was added dropwise to a stirred solution of *n*-BuLi (0.53 mL, 5.3 mmol) in Et_2O (20 mL) at −78 °C. After *ca.* 15 min, diethyl pentafluorophenylboronate (1.34 g, 5.0 mmol) was added dropwise. The mixture was stirred at −78 °C for 20 min, treated with solution of 2 M HCl in Et_2O (2.7 mL, 5.4 mmol), and slowly warmed up to room temperature. After 3 hrs aniline (0.60 g, 6.5 mmol) and salicylaldehyde (0.59 g, 4.8 mmol) were added, and the reaction was stirred for 2 hrs at rt. Then volatiles were removed in vacuo. The resulting yellow oil was dissolved in 5 mL of ethanol and a solid precipitated. It was obtained by filtration of a cooled solution. The bright yellow crystalline solid was washed with cold mixture of Et_2O and hexane, and dried under vacuum. Yield 0.84 g (1.6 mmol, 31 %). M.p. 152-154°C. ^{1}**H NMR** (300 MHz, acetone-d$_6$): δ = 9.23 (s, 1H, N=C**H**), 7.85 (ddd, J_{HH} = 7.8, 1.8, 0.6 Hz, 1H), 7.68 (ddd, J = 8.4, 7.3, 1.8 Hz, 1H), 7.55-7.34 (m, 5H), 7.07 (ddd, J = 7.8, 7.3, 1.0 Hz, 1H), 6.98 (ddt, J = 8.4, 1.0, 0.6 Hz, 1H) ppm. ^{11}**B NMR** (96 MHz, acetone-d$_6$): δ = 1 ($w_{1/2}$ = 130 Hz) ppm. ^{13}**C NMR** (75 MHz, acetone-d$_6$): δ = 166.0 (N=**C**H), 159.8 (**Sal**, O-**C**), 144.0 (**Ani**, N-**C**), 139.9, 133.9, 129.3, 129.2, 123.2, 120.5, 119.1, 118.2 ppm. ^{19}**F NMR** (282 MHz, acetone-d$_6$): δ = −135.02 (dd, J_{FF} = 23.5, 9.2 Hz, 2F), −158.48 (tt, J_{FF} = 20.0, 2.1 Hz, 1F), −165.68 (ddd, J_{FF} = 23.5, 20.0, 9.2 Hz, 2F) ppm. Anal. Calcd for $C_{25}H_{10}BF_{10}NO$

(541.15): C 55.49; H 1.86; N 2.59; F 35.11, found C 54.26; H 2.40; N 2.72%. **UV-Vis**: λ_{max} = 396 nm, ε = 4800 $M^{-1}cm^{-1}$. Fluorescence: λ_{exc} = 396 nm, λ_{em} = 509 nm, Φ = 12%.

DSC analysis. DSC measurements were performed on a DSC Q200 calorimeter from TA Instruments. Melting points (T_m), glass transition temperatures (T_g), and crystallization temperatures (T_c) were established. DSC curves and sample amounts are provided in the Supporting Information (**Table S1**).

X-ray single crystal data collection, reduction and refinement. Single crystals of **1** were obtained through solvent evaporation from para-filmed vials. Single crystal X-ray measurement were performed on a Kuma KM4CCD κ–axis diffractometer with graphite-monochromated Mo K_α radiation (λ = 0.71073 Å) and an Oxford Cryostream cooling device. Data reduction and analysis were carried out with the *CRYSALISPRO* program.[51] Data set was restricted to 0.7 $Å^{-1}$ resolution. The crystal structure was solved using the *SUPERFLIP* program implemented in *CRYSTALS*.[52] The independent atom model (IAM) refinement based on F^2 was performed with the *CRYSTALS* package with $I > -3.0\sigma(I)$ cut-off. Reflections affected by the beam-stop were carefully removed from the refinement. The *Chebychev* (F^2) weights were applied.[53] Atomic scattering factors in their analytical form were taken from the *International Tables for Crystallography*.[54] All non-hydrogen atoms were refined anisotropically and all of the hydrogen atoms were placed in idealized positions within the riding model for atomic displacement parameters (ADPs) (with $U^{H}_{iso} = 1.2 \cdot U^{C}_{eq}$). All hydrogen atoms (with except to the solvent molecules) were clearly visible on the difference density maps. Weighted *R* factors (*wR2*) and all goodness-of-fit (GooF) values are based on F^2. Conventional *R* factors are based on *F* with *F* set to zero for negative F^2. The $F_o^2 > 2\sigma(F_o^2)$ criterion, adopted form *SHELX*, was used only for calculating *R* factors and is not relevant to the choice of reflections for the refinement. The *R* factors based on F^2 are about twice as large as those based on *F*. *DIAMOND*[55] program has been used for visualization. *CHECKCIFs* alert "B" (and "C" alerts) are a consequence of a disordered position of solvent molecules and ambiguity of finding the positions for H-atoms attached to methyl carbon atoms. Solvent molecules are located on symmetry equivalent positions (transformation though 2-fold axis).

Optical measurements. UV-Vis emission spectra were recorded using a Fluorolog 3-2-IHR320-TCSPC (from Jobin Yvon) spectrometer equipped with a photocounter and the CCD detector calibrated with the Spectral Fluorescence Standard Kit (certified by BAM Federal Institute for Materials Research and Testing).[56] All emission data were obtained after excitation at the longest wavelength absorption bands. The absorption spectra were recorded using a Shimadzu RF-5301 PC spectrometer. Quantum yield of emission were determined using known procedures at room temeprature.[2] Coumarine 153 in EtOH was used as the standard for the quantum yield ($\Phi = 38\%$)[57] determination ($c = 5 \times 10^{-6}$ M). Concentration of borinic complexes in their solutions in CH_2Cl_2 was 2×10^{-5} M.

Theoretical calculations. Full geometry optimizations for all compounds were at the RB3LYP/6-31+g(d,p) level of theory. In all cases C-H bond lengths were adjusted to standard neutron distances prior to optimization/single point calculations.[58] Geometries of the excited states along with absorption and emission spectra were obtained using the TD-DFT method with the same basis set starting with the geometries obtained from ground state optimizations. Subsequently, the vibrational frequencies were calculated (for the ground state and for the first excited singlet state) and the results showed that optimized geometries are stable structures. Tight convergence criteria (*opt=tight*) were used along with high precision integrals (*int=UltraFine*) to obtain good quality wave functions. Wave functions were calculated without the use of symmetry constraints (*nosymm*). All calculations were performed using *GAUSSIAN09*[59] suits of programs. *VMD*[60] and *POV-Ray*[61] programs were used for the visualization of molecular orbitals. AIM analysis[62] were done using *AIMall*[46] suits of programs.

Supplementary material. Additional supporting information of this article include: synthetic procedures and details of NMR, X-Ray structure determination, experimental optical properties, computational studies and DSC characterization. CCDC 1035702 contains the supplementary crystallographic data (CIF file) for crystal studied in this work. It can be obtained free of charge from the Cambridge Crystallographic Data Centre *via* www.ccdc.cam.ac.uk/data_request/cif or from the authors.

Acknowledgments. The MPD/2010/4 project is realized within the MPD programme of Foundation for Polish Science, cofinanced from European Union, Regional Development Fund. This work was supported by the Warsaw University of Technology. The support by Aldrich Chemical Co., Milwaukee, WI, U.S.A., through continuous donation of chemicals and equipment is gratefully acknowledged. G.W.B. thanks the Foundation for Polish Science for financial support within the **International PhD Program**. Authors gratefully acknowledge The Interdisciplinary Centre of Mathematical and Computational Modelling in Warsaw (grant no. G33-14) for providing computer facilities on which most of the calculations were done.

References

1 D. Frath, J. Massue, G. Ulrich and R. Ziessel, *Angew. Chem. Int. Ed.*, 2014, **53**, 2290–2310.

2 G. Wesela-Bauman, P. Ciećwierz, K. Durka, S. Luliński, J. Serwatowski and K. Woźniak, *Inorg. Chem.*, 2013, **52**, 10846–10859.

3 Y.-L. Rao and S. Wang, *Inorg. Chem.*, 2011, **50**, 12263–12274.

4 K. Tanaka and Y. Chujo, *Macromol. Rapid Commun.*, 2012, **33**, 1235–1255.

5 Y. Tokoro, A. Nagai and Y. Chujo, *Macromolecules*, 2010, **43**, 6229–6233.

6 Y. Tokoro, A. Nagai and Y. Chujo, *Appl. Organomet. Chem.*, 2010, **24**, 563–568.

7 F. Jäkle, *Chem. Rev.*, 2010, **110**, 3985–4022.

8 A. Nagai and Y. Chujo, *Chem. Lett.*, 2010, **39**, 430–435.

9 F. Jäkle, *Coord. Chem. Rev.*, 2006, **250**, 1107–1121.

10 D. Li, H. Zhang and Y. Wang, *Chem. Soc. Rev.*, 2013, **42**, 8416–8433.

11 J. Massue, D. Frath, P. Retailleau, G. Ulrich and R. Ziessel, *Chem. Eur. J.*, 2013, **19**, 5375–5386.

12 Y. Qin, I. Kiburu, S. Shah and F. Jäkle, *Org. Lett.*, 2006, **8**, 5227–5230.

13 F. Cheng, E. M. Bonder, S. Salem and F. Jäkle, *Macromolecules*, 2013, **46**, 2905–2915.

14 A. Nagai, S. Kobayashi, Y. Nagata, K. Kokado, H. Taka, H. Kita, Y. Suzuri and Y. Chujo, *J. Mater. Chem.*, 2010, **20**, 5196–5201.

15 H. Li and F. Jäkle, *Angew. Chem. Int. Ed.*, 2009, **48**, 2313–2316.

16 Y. Nagata and Y. Chujo, *Macromolecules*, 2008, **41**, 2809–2813.

17 G. Wesela-Bauman, S. Lulinski, J. Serwatowski and K. Wozniak, *Phys. Chem. Chem. Phys.*, 2014, **16**, 22762–22774.

18 G. Wesela-Bauman, S. Parsons, J. Serwatowski and K. Wozniak, *CrystEngComm*, 2014, **16**, 10780–10790.

19 S. Kappaun, S. Rentenberger, A. Pogantsch, E. Zojer, K. Mereiter, G. Trimmel, R. Saf, K. C. Möller, F. Stelzer and C. Slugovc, *Chem. Mater.*, 2006, **18**, 3539–3547.

20 Y. Cui and S. Wang, *J. Org. Chem.*, 2006, **71**, 6485–6496.

21 Y. Cui, Q.-D. Liu, D.-R. Bai, W.-L. Jia, Y. Tao and S. Wang, *Inorg. Chem.*, 2005, **44**, 601–609.

22 Y.-K. Lim, S. Wallace, J. C. Bollinger, X. Chen and D. Lee, *Inorg. Chem.*, 2007, **46**, 1694–1703.

23 J. A. Riddle, S. P. Lathrop, J. C. Bollinger and D. Lee, *J. Am. Chem. Soc.*, 2006, **128**, 10986–10987.

24 D. Frath, S. Azizi, G. Ulrich and R. Ziessel, *Org. Lett.*, 2012, **14**, 4774–4777.

25 D. Frath, S. Azizi, G. Ulrich, P. Retailleau and R. Ziessel, *Org. Lett.*, 2011, **13**, 3414–3417.

26 G. Wesela-Bauman, L. Jastrzębski, P. Kurach, S. Luliński, J. Serwatowski and K. Woźniak, *J. Organomet. Chem.*, 2012, **711**, 1–9.

27 K. Durka, S. Lulinski, G. J. Wesela-Bauman, K. Wozniak, J. Serwatowski, J. Smetek, P. Szczepanik, U. E. Wawrzyniak, I. Glowacki, B. Luszczynska, E. Witkowska and G. Wiosna-Salyga, *J. Mater. Chem. C*, 2014, DOI:10.1039/C4TC02350A.

28 Q. Wu, M. Esteghamatian, N.-X. Hu, Z. Popovic, G. Enright, Y. Tao, M. D'Iorio and S. Wang, *Chem. Mater.*, 2000, **12**, 79–83.

29 F. Cheng, E. M. Bonder, A. Doshi and F. Jakle, *Polym. Chem.*, 2012, **3**, 596–600.

30 F. Cheng and F. Jakle, *Chem. Commun.*, 2010, **46**, 3717–3719.

31 F. Cheng, E. M. Bonder and F. Jäkle, *Macromolecules*, 2012, **45**, 3078–3085.

32 P. Hewavitharanage, P. Nzeata and J. Wiggins, *Eur. J. Chem.*, 2012, **3**, 13–16.

33 H. Li and F. Jäkle, *Macromolecules*, 2009, **42**, 3448–3453.

34 C. Hansch, A. Leo and R. W. Taft, *Chem. Rev.*, 1991, **91**, 165–195.

35 E. V. Anslyn and D. A. Dougherty, *Modern Physical Organic Chemistry*, University Science, 2006.

36 A. Echevarria, M. da G. Nascimento, V. Geronimo, J. Miller and A. Giesbrecht, *J. Braz. Chem. Soc.*, 1999, **10**, 60 – 64.

37 S. L. Hellstrom, J. Ugolotti, G. J. P. Britovsek, T. S. Jones and A. J. P. White, *New J. Chem.*, 2008, **32**, 1379–1387.

38 J. Ugolotti, S. Hellstrom, G. J. P. Britovsek, T. S. Jones, P. Hunt and A. J. P. White, *Dalton Trans.*, 2007, 1425–1432.

39 L. Wang, Z. Zhang, X. Cheng, K. Ye, F. Li, Y. Wang and H. Zhang, *J. Mater. Chem. C*, 2015, DOI: 10.1039/C4TC02070G.

40 R. Pohl and P. Anzenbacher, *Org. Lett.*, 2003, **5**, 2769–2772.

41 R. Pohl, V. A. Montes, J. Shinar and P. Anzenbacher, *J. Org. Chem.*, 2004, **69**, 1723–1725.

42 V. A. Montes, R. Pohl, J. Shinar and P. Anzenbacher, *Chem. – Eur. J.*, 2006, **12**, 4523–4535.

43 N. Agarwal, P. K. Nayak, F. Ali, M. P. Patankar, K. L. Narasimhan and N. Periasamy, *Synth. Met.*, 2011, **161**, 466 – 473.

44 V. A. Montes, G. Li, R. Pohl, J. Shinar and P. Anzenbacher, *Adv. Mater.*, 2004, **16**, 2001–2003.

45 S. Chibani, A. Charaf-Eddin, B. Le Guennic and D. Jacquemin, *J. Chem. Theory Comput.*, 2013, **9**, 3127–3135.

46 T. A. Keith, *AIMAll*, TK Gristmill Software, Overland Park KS, USA, 2012.

47 *OriginPro*, OriginLab, Northampton, MA.

48 J. R. Lakowicz, *Principles of Fluorescence Spectroscopy*, Kluwer Academic/Plenum Publishers, Second., 1999.

49 K. Durka, R. Kaminski, S. Lulinski, J. Serwatowski and K. Wozniak, *Phys. Chem. Chem. Phys.*, 2010, **12**, 13126–13136.

50 J. Peyton III, *J. Organomet. Chem.*, 1978, **156**, 101 – 110.

51 *CrysAlis Pro Software*, Agilent Technologies, 2010.

52 P. W. Betteridge, J. R. Carruthers, R. I. Cooper, K. Prout and D. J. Watkin, *J. Appl. Crystallogr.*, 2003, **36**, 1487.

53 J. R. Carruthers and D. J. Watkin, *Acta Crystallogr. Sect. A*, 1979, **35**, 698–699.

54 H. Fuess (Ed.), *International Tables for Crystallography,Mathematical, Physical and Chemical Tables*, Chester, 2006, vol. C.

55 H. Putz and K. Brandenburg, *Diamond - Crystal and Molecular Structure Visualization*, Germany, 2012.

56 D. Pfeifer, K. Hoffmann, A. Hoffmann, C. Monte and U. Resch-Genger, *J. Fluoresc.*, 2006, **16**, 581–587.

57 A. M. Brouwer, *Pure Appl. Chem.*, 2011, **83**, 2213–2228.

58 F. H. Allen and I. J. Bruno, *Acta Crystallogr. Sect. B*, 2010, **66**, 380–386.

59 M. J. Frisch, G. W. Trucks, H. B. Schlegel, G. E. Scuseria, M. A. Robb, J. R. Cheeseman, G. Scalmani, V. Barone, B. Mennucci, G. A. Petersson, H. Nakatsuji, M. Caricato, X. Li, H. P. Hratchian, A. F. Izmaylov, J. Bloino, G. Zheng, J. L. Sonnenberg, M. Hada, M. Ehara, K. Toyota, R. Fukuda, J. Hasegawa, M. Ishida, T. Nakajima, Y. Honda, O. Kitao, H. Nakai, T. Vreven, J. A. Montgomery, Jr., J. E. Peralta, F. Ogliaro, M. Bearpark, J. J. Heyd, E. Brothers, K. N. Kudin, V. N. Staroverov, T. Keith, R. Kobayashi, J. Normand, K. Raghavachari, A. Rendell, J. C. Burant, S. S. Iyengar, J. Tomasi, M. Cossi, N. Rega, J. M. Millam, M. Klene, J. E. Knox, J. B. Cross, V. Bakken, C. Adamo, J. Jaramillo, R. Gomperts, R. E. Stratmann, O. Yazyev, A. J. Austin, R. Cammi, C. Pomelli, J. W. Ochterski, R. L. Martin, K. Morokuma, V. G. Zakrzewski, G. A. Voth, P. Salvador, J. J.

Dannenberg, S. Dapprich, A. D. Daniels, O. Farkas, J. B. Foresman, J. V. Ortiz, J. Cioslowski, and D. J. Fox, *Gaussian 09*, Gaussian, Inc, Wallingford CT, 2010.
60 W. Humphrey, A. Dalke and K. Schulten, *J. Mol. Graph.*, 1996, **14**, 33 – 38.
61 *Persistence of Vision Raytracer (Version 3.6)*, Persistence of Vision Pty. Ltd., 2004.
62 R. F. W. Bader, *Atoms in Molecules: A Quantum Theory*, Oxford University Press, Oxford, 1990.